

Functional Hyperbranched Polymers: Toward Targeted *in Vivo* ^{19}F Magnetic Resonance Imaging Using Designed Macromolecules

Kristofer J. Thurecht,[†] Idriss Blakey,[†] Hui Peng,[†] Oliver Squires,[†] Steven Hsu,[†] Cameron Alexander,[‡] and Andrew K. Whittaker^{*,†}

Australian Institute for Bioengineering and Nanotechnology and Centre for Advanced Imaging, University of Queensland, St. Lucia, QLD, 4072, Australia and School of Pharmacy, University of Nottingham, Nottingham, NG7 2RD, U.K.

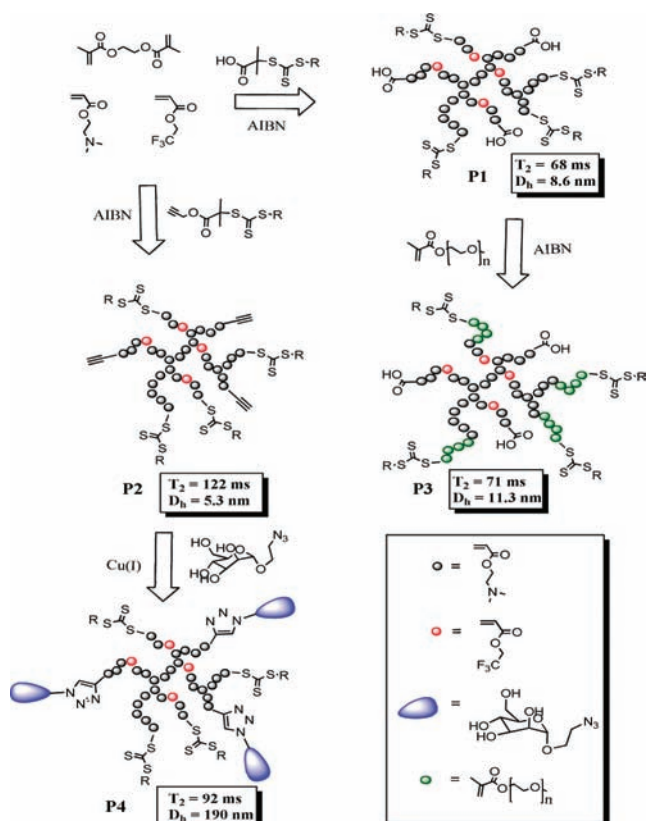
Received January 11, 2010; E-mail: a.whittaker@uq.edu.au

Accurate and early diagnosis of diseases, such as cancer, is the “holy grail” of medical imaging. Techniques, such as computed axial tomography, magnetic resonance imaging (MRI), ultrasound etc., are able to detect various diseases, but often the detection limits mean the diseases have progressed beyond acceptable recovery. Early detection requires imaging techniques with higher sensitivity, while maintaining specificity for disease states (e.g., tumors). We report on our recent efforts in developing sensitive polymeric ^{19}F MRI contrast agents that combine controllable functionality, ability for cell targeting, and low cytotoxicity.

Recent synthetic advances that facilitate intimate control over polymer structure and functionality have led to the advent of polymeric theranostics, nanomedical devices for diagnosis and treatment of diseases.¹ Monitoring these devices in an *in vivo* clinical setting remains a significant scientific challenge, despite some elegant attempts to develop polymeric devices^{2–4} or emulsions^{5,6} for ^{19}F MRI. No system to date has demonstrated the ability to be both easily and universally functionalized, while exhibiting high ^{19}F MRI sensitivity. Poor sensitivity is attributed to three main factors:⁴ poor molecular mobility, association of the fluorinated segments, and low fluorine content. To overcome such issues, our approach uses hyperbranched polymers enabling high segmental molecular mobility to be achieved while maintaining high fluorine content. Controlled functionality was introduced through reversible addition–fragmentation chain transfer (RAFT) chemistry, and molecular mobility was conferred via low- T_g (acrylate) and polar repeat units that are well hydrated under aqueous conditions. Random branching frustrates aggregation of the fluorinated segments allowing incorporation of up to 20 mol % fluoro-monomer. The “shape-persistence” of the hyperbranched molecule means that orientation of functionality, such as cell-targeting agents, can be controlled thus ensuring correct presentation for efficient biological recognition if required.

The hyperbranched polymers were synthesized using a variant of published RAFT routes⁷ (Scheme 1). 2-Dodecylsulfanyl thiocarbonyl sulfanyl-2-methylpropionic acid and the alkyne-terminated derivative⁸ were employed as RAFT agents. A statistical, hyperbranched polymer of dimethylaminoethylacrylate (DMAEA, 77 mol %) and trifluoroethyl acrylate (tFEA, 19 mol %) was synthesized using ethyleneglycol dimethacrylate (EGDMA, 4 mol %) as a branching agent. Details of the synthesis and polymer properties are given in the Supporting Information (SI, Table S1). The size of the hyperbranch particles was measured using DLS in pure water (Scheme 1). Except for the mannose-derivative (P4), the particles were in the range of 10 nm. This suggests they exist as discrete macromolecules in solution while P4 forms agglomerated particles. Nonetheless, the ^{19}F T_2 relaxation times at 7 T (20 mg/mL) varied little between the different polymers irrespective of their structure (Scheme 1; details in SI).

Scheme 1. Synthetic Scheme and Physical Properties of Polymers Having Acid (P1), Alkyne (P2), and Mannose (P4) End Groups



The RAFT end groups were removed using an approach reported by Perrier et al.⁹ Initial tests to establish the cytocompatibility of the polymers and degradation products likely to arise under physiological conditions showed that P1 exhibited significant cytotoxicity compared to a control polymer (PEG-400) as evaluated by the MTS assay.¹⁰ We attribute this to interactions between the solubilizing cationic pendant groups with cells,¹¹ rather than from degradation products of the RAFT end group;¹² successful removal of the RAFT end groups and polymer purity were established by UV–vis spectroscopy and ^1H NMR. Chain extension of P1 with polyethyleneglycol monomethylether methacrylate (PEGMA) resulted in a mobile polycation core with pendant PEGMA arms (P3, Scheme 1). Cell proliferation assays showed that P3 exhibited considerably lower cytotoxicity than P1 and was generally statistically the same as the nontoxic control, PEG(400). This suggests that the PEGMA chains shielded the hyperbranched core, decreasing the toxic effect of the cations.

Having established the cytocompatibility afforded by the outer PEGMA “shield”, we sought to demonstrate the ease of function-

[†] University of Queensland.

[‡] University of Nottingham.

alization, such that the parent hyperbranched polymers might be adaptable to a variety of biological targets. We chose mannose as a representative ligand to attach to the hyperbranched polymers since mannose-binding lectins (MBL) play an important physiological role in immune response through processes such as opsonization. Accordingly, P2 was conjugated with mannose derivatives via Huisgen-type “click” chemistry (Scheme 1), and the selectivity of binding was investigated by *in vitro* testing. ^1H NMR and GPC-MALS indicated that P2 had approximately four pendent alkyne moieties (Table S1). Following addition of mannose azide¹³ in the presence of CuSO_4 and sodium ascorbate, the final hyperbranched molecule (P4) was shown by GPC-MALS and ^1H NMR (ESI) to contain, on average, four mannose units, indicating the success of the functionalization procedure.

The accessibility and presentation of the mannose ligands was determined using an established binding assay.¹³ We qualitatively compared the binding efficiency of P2 and P4 with Concanavalin A, a model mannose-binding ligand (details in SI). P2 exhibited no change in absorbance over 1 h, whereas P4 showed an increase in absorbance over 10 min indicating that the MBL was ligating to the mannose groups. By contrast, P4 exhibited no change in absorbance over 1 h when incubated with bovine serum albumen (BSA) as a control protein. These tests confirmed that polymer functionalization was successful and that targeted binding of the polymer via a suitably presented ligand can be achieved through a specific receptor-mediated pathway.

The culminating experiments were designed to establish the potential for these hyperbranched fluoropolymers as a bioimaging platform. The sensitivity of the ^{19}F image is a function of both concentration (spin density) of ^{19}F atoms and the T_2 relaxation time of the polymer (molecular mobility).⁴ We intended to optimize both parameters through the hyperbranched polymer structure. The long ^{19}F transverse (T_2) relaxation time of P1 was measured in the high-field animal imaging instrument using a spin echo pulse sequence and was found to be 88 ms at 16.4 T at a concentration of 20 mg/mL in pure water. The longitudinal relaxation time (T_1) was 480 ms. Using a spin-echo 3D imaging pulse sequence, we investigated the effect of concentration of a polymer solution on the signal-to-noise ratio (S/N) of the image (solution in a 5 mL vial, SI). 36 accumulations were acquired with a total imaging time of ~ 8 min. The S/N ratio increased linearly with polymer concentration over the range 5–20 mg/mL suggesting that the image intensity was only dependent on the fluorine concentration and that the T_2 relaxation time did not change over these concentration ranges; the dipolar couplings experienced by the fluorine nuclei across this concentration range remained unchanged. These results show that our polymers exhibit high sensitivity and images can be obtained within short acquisition times; to our knowledge, such high sensitivity has not been reported for polymeric systems.

We finally tested the viability of our hyperbranched polymers for *in vivo* ^{19}F MRI, using the “platform” polymer P1. This polymer was specifically chosen because it was nontargeting and, thus, would not be expected to accumulate selectively in nonexcretory organs after injection. Accordingly, a 100 μL solution of P1 (20 mg/mL) was injected into the tail vein of a mouse. 30 min following injection, minimal ^{19}F image intensity was detected due to dispersion of P1 throughout the vasculature. However, after 2 h a high resolution ^1H MR image was taken of the lower abdominal area of the mouse, followed immediately by a ^{19}F MR image of the same region (full details of conditions are provided in SI). Figure 1 shows an overlay of the ^1H and ^{19}F images 2 h after P1 injection. In the frontal slice, the bladder and intestine are clearly delineated while a slice through the

transverse direction shows the spinal column and bladder. In both cases, the ^{19}F signal was clearly observed, predominantly within the bladder. This suggests that we are able to successfully image these polymers *in vivo* and that the blood-borne polymer can be excreted by kidneys. This is the first example of functionalizable copolymers successfully engineered for *in vivo* ^{19}F MRI.

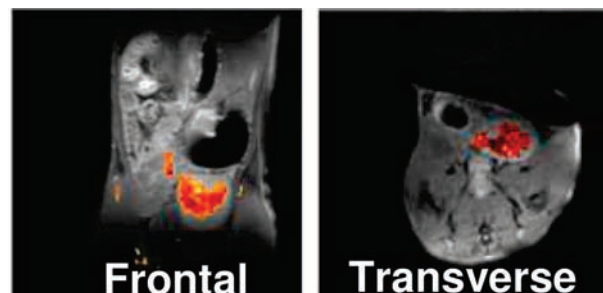


Figure 1. MRI images of mouse abdominal region 2 h following injection of P1 into mouse tail vein. ^1H image is shown in greyscale while ^{19}F image is overlaid. P1 appears accumulated in the bladder.

In conclusion, we have demonstrated the design and synthesis of hyperbranched molecules that can be successfully imaged *in vivo* using ^{19}F MRI in under 10 min. These polymers are cytocompatible following chain extension with PEGMA. In addition, functionalization of these macromolecules can be achieved in a facile manner and with accessible and correct ligand presentation. Such hyperbranched polymers hold promise as new generation tracking and targeting MRI contrast agents; further tests on the *in vivo* efficiency of a variety of specific cell-targeted polymers are currently underway in our laboratory.

Acknowledgment. The authors thank Dr. Nyoman Kurniawan (Centre for Advanced Imaging), Dr. Lauren Butler (Australian National Fabrication Facility), and Dr. Barbara Rolfe (Australian Institute for Bioengineering and Nanotechnology). Funding was received from the Queensland State Government (NIRAP) and the Australian Research Council (DP1094205).

Supporting Information Available: Full synthetic procedures, characterization, and analyses of polymers; NMR/MRI parameters. This material is available free of charge via the Internet at <http://pubs.acs.org>.

References

- (1) Weissleder, R.; Pittet, M. J. *Nature* **2008**, *452*, 580–589.
- (2) Nystrom, A. M.; Bartels, J. W.; Du, W.; Wooley, K. L. *J. Polym. Sci., Part A: Polym. Chem.* **2009**, *47*, 1023–1037.
- (3) Du, W.; Nystrom, A. M.; Zhang, L.; Powell, K. T.; Li, Y.; Cheng, C.; Wickline, S. A.; Wooley, K. L. *Biomacromolecules* **2008**, *9*, 2826–2833.
- (4) Peng, H.; Blakey, I.; Dargaville, B.; Rasoul, F.; Rose, S.; Whittaker, A. K. *Biomacromolecules* **2009**, *10*, 374–381.
- (5) Janjic, J. M.; Srinivas, M.; Kadayakkara, D. K. K.; Ahrens, E. T. *J. Am. Chem. Soc.* **2008**, *130*, 2832–2841.
- (6) Ahrens, E. T.; Flores, R.; Xu, H.; Morel, P. A. *Nat. Biotechnol.* **2005**, *23*, 983–987.
- (7) Liu, B.; Kazlauciusas, A.; Guthrie, J. T.; Perrier, S. *Macromolecules* **2005**, *38*, 2131–2136.
- (8) Quemener, D.; Davis, T. P.; Barner-Kowollik, C.; Stenzel, M. H. *Chem. Commun.* **2006**, 5051–5053.
- (9) Perrier, S.; Takolpuckdee, P.; Mars, C. A. *Macromolecules* **2005**, *38*, 2033–2036.
- (10) Cory, A. H.; Owen, T. C.; Barltrop, J. A.; Cory, J. G. *Cancer Commun.* **1991**, *3*, 207–12.
- (11) Lv, H.; Zhang, S.; Wang, B.; Cui, S.; Yan, J. J. *Controlled Release* **2006**, *114*, 100–109.
- (12) Chang, C.-W.; Bays, E.; Tao, L.; Alconcel, S. N. S.; Maynard, H. D. *Chem. Commun.* **2009**, 3580–3582.
- (13) Geng, J.; Mantovani, G.; Tao, L.; Nicolas, J.; Chen, G.; Wallis, R.; Mitchell, D. A.; Johnson, B. R. G.; Evans, S. D.; Haddleton, D. M. *J. Am. Chem. Soc.* **2007**, *129*, 15156–15163.

JA100252Y